

---

# Applications of Differentiable Physics Simulations in Particle Accelerator Modeling

---

**Ryan Roussel**

SLAC National Accelerator Laboratory  
Menlo Park, CA 94025  
rroussel@slac.stanford.edu

**Auralee Edelen**

SLAC National Accelerator Laboratory  
Menlo Park, CA 94025  
edelen@slac.stanford.edu

## Abstract

Current physics models used to interpret experimental measurements of particle beams require either simplifying assumptions to be made in order to ensure analytical tractability, or black box optimization methods to perform model based inference. This reduces the quantity and quality of information gained from experimental measurements, in a system where measurements have a limited availability. However differentiable physics modeling, combined with machine learning techniques, can overcome these analysis limitations, enabling accurate, detailed model creation of physical accelerators. Here we examine two applications of differentiable modeling, first to characterize beam responses to accelerator elements exhibiting hysteretic behavior, and second to characterize beam distributions in high dimensional phase spaces.

## 1 Introduction

Particle accelerators are indispensable tools for making discoveries in the physical, material, chemical and biological sciences. Detailed physics models have been developed to describe the generation and manipulation of particle beams for these applications. Despite this wealth of knowledge, accurately replicating realistic conditions in the physical accelerator is challenging due to the limited availability of measurements and the complex nature of real accelerator components and beam distributions. In this work, we examine the application of differentiable computing techniques combined with machine learning towards enabling detailed, accurate modeling of realistic accelerator elements and beam properties.

## 2 Hysteresis Modeling

Hysteresis is a well-known physical phenomenon where the state of a given system is dependent on its historical path through state-space. Hysteresis effects in magnetic [1], mechanical [2] and material [3] elements of particle accelerators makes optimizing the performance of current accelerator facilities used for scientific discovery challenging using standard black box optimization algorithms, such as Bayesian optimization (BO) [4].

The Preisach model [5, 6] is a numerical representation of hysteresis, comprised of a discrete set of *hystérons*, which when added together, model the output of a hysteretic system  $f(t)$  for a time dependent input  $u(t)$ . Given a set of discrete time ordered inputs  $u_i = u(t_i)$ , the hysteron state is represented by the hysteron operator  $\hat{\gamma}_{\alpha\beta}$  shown in Fig. 1a, which has an output of  $\pm 1$ , where  $\alpha$  and  $\beta$  describe the input required to switch the hysteron between its two possible states. The number of hystérons with values  $(\alpha, \beta)$  is given by the hysteron density function  $\mu(\alpha, \beta)$ , plotted on the Preisach  $(\alpha-\beta)$  plane (Fig. 1b).

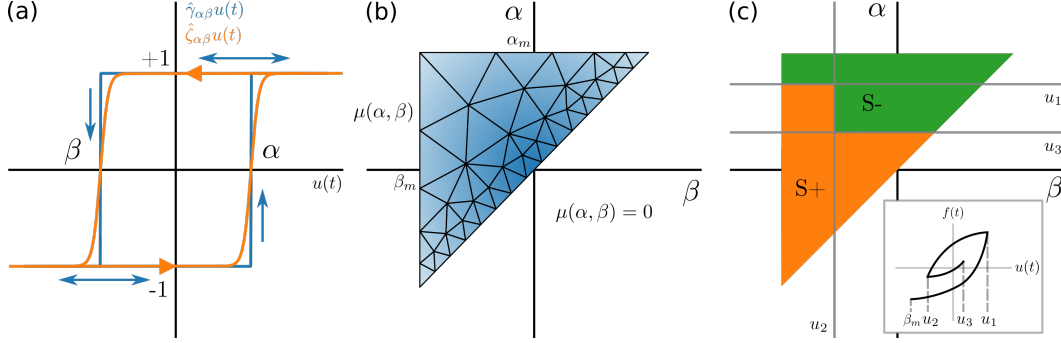


Figure 1: Elements of the differentiable non-parametric Preisach hysteresis model. (a) Output of the hysteron operator  $\hat{\gamma}_{\alpha\beta}$  and the approximate differentiable hysteron operator  $\hat{\zeta}_{\alpha\beta}$  acting on the input  $u(t)$ . (b) Discretization of the density on the Preisach  $(\alpha$ - $\beta)$  plane. Note that  $\mu(\alpha, \beta) = 0$  if  $\alpha < \beta$ ,  $\alpha > \alpha_m$  or  $\beta < \beta_m$  where  $\alpha_m, \beta_m$  are equal to the maximum and minimum inputs of the model respectively. (c)  $S^+$  and  $S^-$  sub-domains after three time steps, where  $u_1 > u_3 > u_2 > \beta_m$ , assuming that all hysterons are in the negative state initially. Inset: Corresponding model output.

The Preisach model output is represented by

$$f(t) = \hat{\Gamma}u(t) = \iint_{\alpha \geq \beta} \mu(\alpha, \beta) \hat{\gamma}_{\alpha\beta} u(t) d\alpha d\beta \quad (1)$$

where  $\alpha \geq \beta$  results from physical conditions of the hysteron operator. This integral is evaluated through a geometric interpretation, shown in Fig. 1(c). Given the sequence of input values  $u_i$ , we can determine sub-regions of the Preisach plane,  $S^+$  and  $S^-$ , where hysteron operators output positive and negative states respectively using a geometric interpretation.

Fitting a Preisach model to experimental data requires the determination of the hysteron density function  $\mu(\alpha, \beta)$ , often referred to as the *identification problem*. We discretize the hysteron density function onto a fine mesh  $\mu_i = \mu(\alpha_i, \beta_i)$  and treat the density at each mesh point as a free tuning parameter to fit experimental measurements. Due to the large number of mesh points and corresponding free parameters, gradient enabled optimization must be used to fit the model to experimental measurements. This is achieved by implementing the Preisach hysteresis calculation in PyTorch [7], which uses backwards auto-differentiation to efficiently calculate gradients.

Our goal is to determine hysteresis properties from beam-based measurements, so we combine the differentiable hysteresis model with a Gaussian process (GP) model [8], implemented in GPyTorch [9], to describe beam propagation as a function of magnetic fields due to hysteresis. We simultaneously infer hysteresis model parameters and GP hyperparameters from training data by maximizing a differentiable calculation of the log likelihood with respect to the parameters of the joint model through gradient descent.

We demonstrate the effectiveness of our joint hysteresis-GP (H-GP) model by fitting the beam response with respect to the current applied to a focusing magnet located in the Advanced Photon Source (APS) injector [10]. Measurements from this experiment, shown in Fig. 2, have two sources of uncertainty, one from random noise inherent in the accelerator (aleatoric uncertainty) and one due to the unknown properties of magnetic hysteresis (epistemic uncertainty). We trained two models on the entire data set using L-BFGS with gradient information, the results of which are shown in Fig. 2. First, we trained a normal GP model (Fig. 2a) which does not take into account the existence of hysteresis. As a result it interprets epistemic errors due to hysteresis as aleatoric uncertainty, overestimating uncertainties in portions of the input domain. However, the joint hysteresis-GP model (Fig. 2b), is able to resolve hysteresis cycles inside the data, removing epistemic uncertainties in the model prediction, thus improving model accuracy and reducing uncertainty. The increase in accuracy from joint hysteresis-GP models has ramifications for model-based, online optimization of accelerators using BO [11].

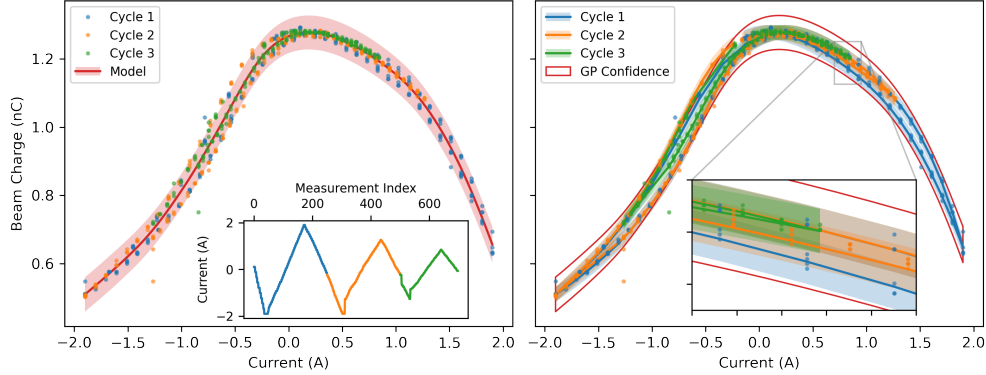


Figure 2: Comparison between GP modeling and joint hysteresis-GP modeling of beam transmission as a function of quadrupole current at the APS injector. (Left) GP model prediction with training data over three cycles (see inset). Shading denotes  $2\sigma$  confidence region. (Right) Hysteresis-GP model prediction, colored by cycle index, compared to confidence interval of normal GP model.

### 3 Phase Space Reconstruction

Tomographic measurement techniques are used in accelerators to determine the density distribution of beam particles in phase space  $\rho(x, p_x, y, p_y, z, p_z)$  from limited measurements [12, 13, 14, 15, 16, 17]. While these methods have been shown to effectively reconstruct 2D phase spaces from image projections using algebraic methods, application to higher-dimensional spaces requires independence assumptions between the phase spaces of principal coordinate axes  $(x, y, z)$ , complicated phase space rotation procedures [18], or measurement of multiple 2D sub-spaces with specialized diagnostic hardware [19]. It is also possible to directly fit a beam distribution to experimental data through the use of black box optimization algorithms [20, 21, 22] and particle tracking simulations. This however increases the computational cost of inferring the beam distribution from simulation, resulting in simplified beam representations to keep costs within a fixed computational budget.

We propose reducing the computational cost of determining beam phase space distributions by combining methods for parameterizing arbitrary beam probability distributions in 6D phase space using neural networks with differentiable particle tracking simulations. Particle tracking simulations propagate samples from the initial beam distribution down a model of the beamline to simulated diagnostics. This allows us to learn the beam distribution from arbitrary downstream accelerator measurements [23]. Our beam distribution parameterization is heavily inspired by normalizing flows [24], however we are only concerned with forward transformations of drawn samples from a base distribution, and not the transformed probability distribution itself (which requires invertible transformations). Thus we use simple densely connected neural networks instead of a series of invertible transformations.

Fitting neural network parameters to experimental measurements is done by minimizing a loss function to determine the most likely initial beam distribution, subject to the constraint that it reproduces experimental measurements, similar to the maximum entropy tomography algorithm [25]. The likelihood of an initial beam distribution in phase space is maximized by maximizing the distribution entropy, which is proportional to the log of the 6D beam emittance  $\varepsilon_{6D}$  [26]. Thus, we specify a loss function that minimizes the negative entropy of the proposal beam distribution, penalized by the degree to which the proposal distribution reproduces measurements of the transverse beam distribution at the screen location. To evaluate the penalty for a given proposal distribution, we track the proposal distribution through a batch of accelerator simulations that mimic experimental conditions to generate a set of simulated images  $Q_n^{(i,j)}$  to compare with experimental measurements.

As in the previous example, a loss function that is *differentiable* is needed to fit the large number of neural network parameters. Unfortunately, no particle tracking codes which are differentiable with respect to particle coordinates currently exist. To satisfy this requirement, we implement particle tracking and image creation using *PyTorch* [7]. We demonstrated reconstruction of a beam in phase

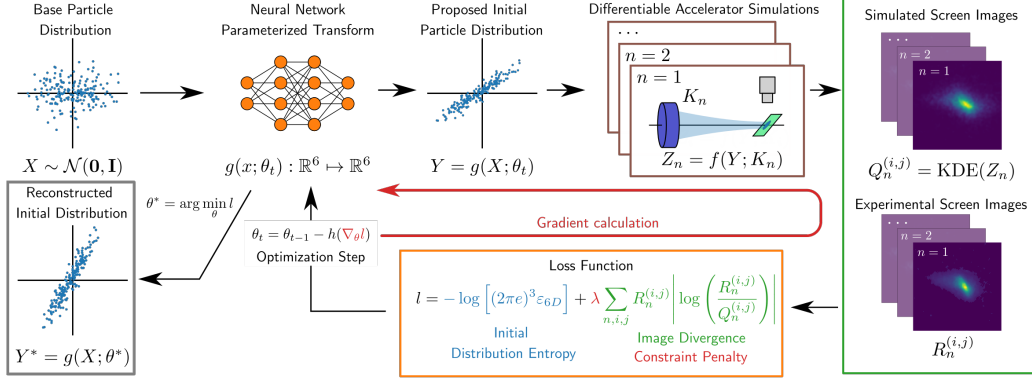


Figure 3: Description of our approach for reconstructing 6D phase space beam distributions. First, a base distribution is transformed via a neural network, parameterized by  $\theta$ , into a proposed initial distribution. This distribution is then transported through a differentiable accelerator simulation of the tomographic beamline. The quadrupole is scanned to produce a series of images on the screen, both in simulation and on the operating accelerator. The images produced both from the simulation  $Q_n^{(i,j)}$  and the accelerator  $R_n^{(i,j)}$  are then compared with a custom loss function, which when optimized, maximizes the entropy of the proposal distribution constrained on accurately reproducing experimental measurements.

space using a synthetic test case, shown in Fig. 4. We see excellent agreement between the average reconstructed and synthetic projections in both transverse correlated and uncorrelated phase spaces, as well as transverse beam images.

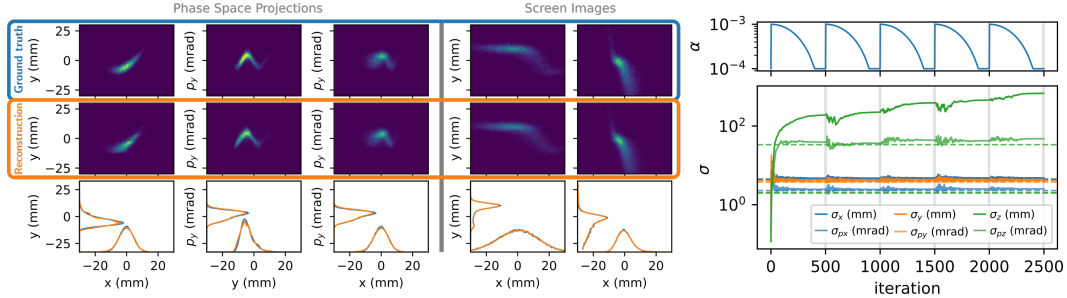


Figure 4: (Left) Comparisons between the synthetic and reconstructed beam probability distributions using our method. A synthetic beam with a tailored phase space distribution is transported through a simulated diagnostic beamline with varying quadrupole strengths and reconstructed using our algorithm. (Right, top) Learning rate schedule for snapshot ensembling. (Right, bottom) Evolution of the proposal distribution beam size in each phase space coordinate during training in synthetic case. Dotted lines denote ground truth values. Vertical lines denote snapshot locations.

We characterize the confidence of our reconstruction using snapshot ensembling [27]. This encourages the optimizer to find multiple possible solutions (if they exist). It is instructive to examine the evolution of the proposal distribution during model training (shown in Fig. 4). The phase space components that have the strongest impact on beam transport through the beamline as a function of quadrupole strength converge quickly, whereas the ones that have little-to-no impact (e.g. the longitudinal distribution characteristics) do not. In particular, we observe that each snapshot converges to beam distributions which have slightly varying energy spreads, signifying uncertainty in that aspect of the beam's phase space, likely due to weak coupling between energy spread and transverse beam size through chromatic aberrations in the quadrupole. The convergence of the proposal distribution thus provides a useful indicator of which components of the phase space can be reliably reconstructed for arbitrary (possibly unknown) tomographic beamlines.

## 4 Conclusion

Here we have shown the advances in accelerator modeling that can be achieved with differentiable computations. When coupled with machine learning techniques these models can surpass limitations faced by historically used methods for analyzing experimental data. Further investments in creating fully differentiable accelerator physics simulations will continue to improve model detail and accuracy.

## 5 Impact Statement

This work is expected to have significant impact on the ability of accelerator diagnostics in the future. As the work is limited within the scope of accelerator science we expect there to be no ethical aspects or future societal impacts beyond the improvement of accelerator operations.

## References

- [1] N. J. Sammut, H. Burkhardt, S. M. White, C. Giloux, and W. Venturini-Delsolaro, “Measurement and Effects of the Magnetic Hysteresis on the LHC Crossing Angle and Separation Bumps,” Aug. 2008. Number: LHC-PROJECT-Report-1107.
- [2] N. Huque, M. Abdelwhab, E. Daly, and Y. Pischalnikov, “Accelerated Life Testing of LCLS-II Cavity Tuner Motor,” in *17th International Conference on RF Superconductivity*, p. THPB062, 2015.
- [3] D. A. Turner, G. Burt, and T. Junginger, “No DC superheating and increased surface pinning in low temperature baked niobium,” tech. rep., Jan. 2022. ISSN: 2693-5015 Type: article.
- [4] J. Snoek, H. Larochelle, and R. P. Adams, “Practical Bayesian Optimization of Machine Learning Algorithms,” in *Advances in Neural Information Processing Systems 25* (F. Pereira, C. J. C. Burges, L. Bottou, and K. Q. Weinberger, eds.), pp. 2951–2959, Curran Associates, Inc., 2012.
- [5] I. D. Mayergoyz and G. Friedman, “Generalized Preisach model of hysteresis,” *IEEE Transactions on Magnetics*, vol. 24, pp. 212–217, Jan. 1988. Conference Name: IEEE Transactions on Magnetics.
- [6] G. Bertotti and I. D. Mayergoyz, eds., *The science of hysteresis*. Amsterdam ; Boston: Academic, 1st ed ed., 2006.
- [7] A. Paszke, S. Gross, F. Massa, A. Lerer, J. Bradbury, G. Chanan, T. Killeen, Z. Lin, N. Gimeshein, L. Antiga, A. Desmaison, A. Kopf, E. Yang, Z. DeVito, M. Raison, A. Tejani, S. Chilamkurthy, B. Steiner, L. Fang, J. Bai, and S. Chintala, “PyTorch: An Imperative Style, High-Performance Deep Learning Library,” in *Advances in Neural Information Processing Systems 32* (H. Wallach, H. Larochelle, A. Beygelzimer, F. d. Alché-Buc, E. Fox, and R. Garnett, eds.), pp. 8024–8035, Curran Associates, Inc., 2019.
- [8] C. E. Rasmussen and C. K. I. Williams, “Bayesian Regression and Gaussian processes,” *Gaussian Processes for Machine Learning*, p. Chapter 2, 2006. ISBN: 026218253X.
- [9] J. R. Gardner, G. Pleiss, D. Bindel, K. Q. Weinberger, and A. G. Wilson, “GPYtorch: Blackbox Matrix-Matrix Gaussian Process Inference with GPU Acceleration,” in *Advances in Neural Information Processing Systems*, 2018.
- [10] Y. Sun, M. Borland, G. I. Fystro, X. Huang, and H. Shang, “Recent Operational Experience with Thermionic RF Guns at the APS,” in *Proc. 12th Int. Particle Accelerator Conf. (IPAC’21)*, pp. 3959–3962, JACoW Publishing, May 2021.
- [11] R. Roussel, A. Edelen, D. Ratner, K. Dubey, J. Gonzalez-Aguilera, Y. Kim, and N. Kuklev, “Differentiable Preisach Modeling for Characterization and Optimization of Particle Accelerator Systems with Hysteresis,” *Physical Review Letters*, vol. 128, p. 204801, May 2022. Publisher: American Physical Society.
- [12] C. McKee, P. O’Shea, and J. Madey, “Phase space tomography of relativistic electron beams,” *Nuclear Instruments and Methods in Physics Research Section A: Accelerators, Spectrometers, Detectors and Associated Equipment*, vol. 358, no. 1, pp. 264–267, 1995.

- [13] S. Hancock, M. Lindroos, E. McIntosh, and M. Metcalf, “Tomographic measurements of longitudinal phase space density,” *Computer Physics Communications*, vol. 118, no. 1, pp. 61–70, 1999.
- [14] D. Stratakis, R. A. Kishek, I. Haber, M. Walter, R. B. Fiorito, S. Bernal, J. Thangaraj, K. Tian, C. Papadopoulos, M. Reiser, and P. G. O’Shea, “Phase space tomography of beams with extreme space charge,” in *2007 IEEE Particle Accelerator Conference (PAC)*, pp. 2025–2029, 2007.
- [15] V. Yakimenko, M. Babzien, I. Ben-Zvi, R. Malone, and X.-J. Wang, “Electron beam phase-space measurement using a high-precision tomography technique,” *Physical Review Special Topics - Accelerators and Beams*, vol. 6, p. 122801, Dec. 2003.
- [16] M. Röhrs, C. Gerth, H. Schlarb, B. Schmidt, and P. Schmüser, “Time-resolved electron beam phase space tomography at a soft x-ray free-electron laser,” *Physical Review Special Topics - Accelerators and Beams*, vol. 12, p. 050704, May 2009.
- [17] M. Gordon, W. Li, M. Andorf, A. Bartnik, C. Duncan, M. Kaemingk, C. Pennington, I. Bazarov, Y.-K. Kim, and J. Maxson, “Four-dimensional emittance measurements of ultrafast electron diffraction optics corrected up to sextupole order,” *Physical Review Accelerators and Beams*, vol. 25, no. 8, p. 084001, 2022.
- [18] K. Hock and A. Wolski, “Tomographic reconstruction of the full 4d transverse phase space,” *Nuclear Instruments and Methods in Physics Research Section A: Accelerators, Spectrometers, Detectors and Associated Equipment*, vol. 726, pp. 8–16, 2013.
- [19] J. C. Wong, A. Shishlo, A. Aleksandrov, Y. Liu, and C. Long, “4D transverse phase space tomography of an operational hydrogen ion beam via noninvasive 2D measurements using laser wires,” *Physical Review Accelerators and Beams*, vol. 25, p. 042801, Apr. 2022.
- [20] M. Wang, Z. Wang, D. Wang, W. Liu, B. Wang, M. Wang, M. Qiu, X. Guan, X. Wang, W. Huang, and S. Zheng, “Four-dimensional phase space measurement using multiple two-dimensional profiles,” *Nuclear Instruments and Methods in Physics Research Section A: Accelerators, Spectrometers, Detectors and Associated Equipment*, vol. 943, p. 162438, Nov. 2019.
- [21] B. Hermann, V. A. Guzenko, O. R. Hürzeler, A. Kirchner, G. L. Orlandi, E. Prat, and R. Ischebeck, “Electron beam transverse phase space tomography using nanofabricated wire scanners with submicrometer resolution,” *Physical Review Accelerators and Beams*, vol. 24, p. 022802, Feb. 2021.
- [22] A. Scheinker, F. Cropp, S. Paiagua, and D. Filippetto, “An adaptive approach to machine learning for compact particle accelerators,” *Scientific reports*, vol. 11, no. 1, pp. 1–11, 2021.
- [23] R. Roussel, A. Edelen, C. Mayes, D. Ratner, J. P. Gonzalez-Aguilera, S. Kim, E. Wisniewski, and J. Power, “Phase space reconstruction from accelerator beam measurements using neural networks and differentiable simulations,” *arXiv preprint arXiv:2209.04505*, 2022.
- [24] I. Kobyzev, S. Prince, and M. Brubaker, “Normalizing flows: An introduction and review of current methods, arxiv e-prints,” *arXiv preprint arXiv:1908.09257*, 2019.
- [25] K. M. Hock and M. G. Ibson, “A study of the maximum entropy technique for phase space tomography,” *Journal of Instrumentation*, vol. 8, pp. P02003–P02003, feb 2013.
- [26] J. Lawson, R. Gluckstern, and P. M. Lapostolle, “Emittance, entropy and information,” *Part. Accel.*, vol. 5, pp. 61–65, 1973.
- [27] G. Huang, Y. Li, G. Pleiss, Z. Liu, J. E. Hopcroft, and K. Q. Weinberger, “Snapshot ensembles: Train 1, get m for free,” *arXiv preprint arXiv:1704.00109*, 2017.